 DOI: 10.17344/acsi.2014.1048

Scientific paper

Stability of the Compounds with the Octahedral $[M^{II}(\kappa^3\text{-}L)_2]$ Coordination Building Blocks of Late 3d Elements *via* Solvate Water Supramolecular Arrangement

Marta Počkaj,* Bojan Kozlevčar and Nives Kitanovski

Faculty of Chemistry and Chemical Technology, University of Ljubljana, Večna pot 113, 1000 Ljubljana, Slovenia.

** Corresponding author: E-mail: marta.pockaj@fkkt.uni-lj.si.*

Received: 23-09-2014

Dedicated to the memory of Prof. Dr. Jurij V. Brenčič.

Abstract

Five new coordination compounds with the common formulae $[M^{II}(bdmpza)_2] \cdot xH_2O$ (bdmpza = bis(3,5-dimethylpyrazol-1-yl)acetate, $C_{11}H_{15}N_4COO^-$; $x = 2$ for Co (**1**), Ni (**2**) and Zn (**3**), $x = 3$ for Mn (**4**) and Fe (**5**)), were synthesized from the reaction mixtures containing appropriate metal salt, bis(3,5-dimethylpyrazol-1-yl)acetic acid-(Hbdmpza), methanol and water. The X-ray single crystal diffraction analysis reveals that all five compounds (**1**–**5**) contain mononuclear homoleptic $[M^{II}(bdmpza)_2]$ coordination molecules, in which the central metal ions are surrounded with two chelating bdmpza ligands. Each ligand is bound tridentately facially *via* κ^3-*N,N,O* sites and centrosymmetric coordination chromophore is thus obtained. In the dihydrates $[M(L)_2] \cdot 2H_2O$, **1**–**3**, every coordination molecule is linked by two water molecules, *i.e.* two pairs of O–H···O hydrogen bonds, on each of the two sides, thus forming infinite chain. In case of the trihydrates $[M(L)_2] \cdot 3H_2O$, **4**–**5**, with an assistance of the additional water molecule, such chains are further connected into extended supramolecular sheets. A stability of both similar hydrate types is confirmed by powder XRD data and IR analysis. The ionic metal radius and the coordination M–O, M–N bonds were related to the void dimension among the coordination molecules of the title $[M^{II}(bdmpza)_2] \cdot xH_2O$.

Keywords: bdmpza; 3d element; hydrates; hydrogen bonding; supramolecular; isostructural

1. Introduction

Although the coordination chemistry of the first row transition metals with bis(3,5-dimethylpyrazol-1-yl)acetate anions (bdmpza) and related ligands has progressed in recent years due to the extensive search for enzyme-mimicking compounds,[1–5] a detailed investigation of CCDC has shown that only a few hydrates with mononuclear coordination cores have been structurally characterized till now.[6] These are hemihydrate of manganese(I), $[Mn(bdmpza)(CO)_3] \cdot 0.5H_2O$,[7] dihydrate of copper(II), $[Cu(bdmpza)_2] \cdot 2H_2O$,[8] and trihydrate of zinc, $[Zn(bdmpza)_2] \cdot 3H_2O$.[9] Outside the family of first row transition metal compounds, hemihydrate of Re(I), $[Re(bdmpza)(CO)_3] \cdot 0.5H_2O$,[7] and trihydrate of magnesium, $[Mg(bdmpza)_2] \cdot 3H_2O$,[10] were reported as well. The small number of such described compounds is in accordance with the fully completed octahedral coordination sphere of the $[M(\kappa^3\text{-}L)_2]$ type with two strongly bound tridentate bdmpza, thus disabling any potential controlled replacement at one or two coordination sites.[2] Despite of no obvious catalytic potential of such compounds, the aqueous medium of isolation and a prospect of possible catalytic activation[11] may suggest increased interest toward this family of compounds. Further investigation into this direction would thus be motivated. Nevertheless, the number of fully characterized $[M(bdmpza)_2] \cdot xH_2O$ compounds is not large enough to draw any unambiguous suggestion about the influences of water molecules, co-crystallized and/or trapped among the coordination moieties, or the specific metal role in $[M^{II}(\kappa^3\text{-}L)_2]$ coordination sphere regarding the coordination species potential activation. This may well be related with a stability of such hydrogen bonding supramolecular networks, especially outside the mother liquid.

Herein we represent five new hydrates, having $[M^{II}(\kappa^3\text{-}L)_2]$ coordination building blocks of the late 3d elements.

2. Experimental

2. 1. Materials and Synthesis

All commercial starting compounds and solvents were of analytical grade quality and used as received. Hbdmpza ($C_{12}H_{16}N_4O_2$) and $[Cu(C_{12}H_{15}N_4O_2)_2] \cdot 2H_2O$ were prepared following previously reported procedures.[8,9]

$[Co(C_{12}H_{15}N_4O_2)_2] \cdot 2H_2O$, **1**. $CoCl_2 \cdot 6H_2O$ (57.5 mg, 0.242 mmol) was added in 3.3 mL of water/methanol 1:10 v/v solution, while Hbdmpza (30.7 mg, 0.124 mmol) in 4.5 mL NaOH (0.033 M). Both mixtures were slightly heated to dissolve the solids. The ligand solution was added dropwise into the pale pink cobalt chloride solution. Pale orange crystals of **1** started to precipitate after two days at ambient temperature. Prior to the filtration, the mixture was left for a week at 8 °C. The crystallites were dried on air for 3 hours. Yield: 85 mg (60%). Anal. Calcd. for $C_{24}H_{34}CoN_8O_6$: C, 48.9%; H, 5.8%; N, 19.0%. Found: C, 49.1%; H, 5.4%; N, 19.0%.$\bar{\nu}_{max}$: 3527 and 3398 (O–H), 1657 and 1615 (COO_{asym}), 1557 (C–N, C=N), 1460 and 1418 (C–H), 1396 (COO_{sym}) cm^{-1}. λ_{max}: 255, 455 (d-d) nm

$[Ni(C_{12}H_{15}N_4O_2)_2] \cdot 2H_2O$, **2**. $Ni(NO_3)_2 \cdot 6H_2O$ (70.3 mg, 0.242 mmol) was added in 9 mL of water/methanol 1:2 v/v solution, while Hbdmpza (30.9 mg, 0.124 mmol) in 4.5 mL NaOH (0.033 M). Both mixtures were slightly heated to dissolve the solids. The ligand solution was added dropwise into the green nickel nitrate solution. Violet crystals of **2** started to appear at ambient temperature after three days. The crystalline product was filtered off and dried on air for 2 hours. Yield: 42 mg (30%). Anal. Calcd. for $C_{24}H_{34}NiN_8O_6$: C, 48.9%; H, 5.8%; N, 19.0%. Found: C, 49.1%; H, 5.6%; N, 19.1%.$\bar{\nu}_{max}$: 3525 and 3393 (O–H), 1658 and 1620 (COO_{asym}), 1559 (C–N, C=N), 1462 and 1418 (C–H), 1398 (COO_{sym}) cm^{-1}. λ_{max}: 254, 345 (shoulder), 569 (d-d) nm.

$[Zn(C_{12}H_{15}N_4O_2)_2] \cdot 2H_2O$, **3**. $Zn(C_2H_3O_2)_2 \cdot 2H_2O$ (52.9 mg, 0.241 mmol) was added in 7.5 mL of water/methanol 2:3 v/v solution, while Hbdmpza (30.0 mg, 0.121 mmol) in 4.5 mL NaOH (0.033 M). Both mixtures were slightly heated to dissolve the solids. The ligand solution was added dropwise into the colourless zinc acetate solution. Colourless crystals of **3** started to appear at ambient temperature after two days. The crystalline product was filtered off and dried on air for 2 hours. Yield: 39 mg (27%). Anal. Calcd. for $C_{24}H_{34}ZnN_8O_6$: C, 48.4%; H, 5.8%; N, 18.8%. Found: C, 47.7%; H, 5.7%; N, 18.1%.$\bar{\nu}_{max}$: 3527 and 3395 (O–H), 1658 and 1621 (COO_{asym}), 1558 (C–N, C=N), 1461 and 1418 (C–H), 1397 (COO_{sym}) cm^{-1}. λ_{max}: 240 nm.

$[Mn(C_{12}H_{15}N_4O_2)_2] \cdot 3H_2O$, **4**. Water (2.25 mL) solution of $MnSO_4 \cdot H_2O$ (40.7 mg, 0.241 mmol) was added dropwise into the methanol (2.25 mL) solution of Hbdmpza (29.4 mg, 0.118 mmol). The colourless solution was left at 8 °C, from which colourless crystals of **4** started to appear after a day. The crystalline product was filtered off and dried on air for 3 hours. Yield: 56 mg (40%). Anal. Calcd. for $C_{24}H_{36}MnN_8O_7$: C, 47.8%; H, 6.0%; N, 18.6%. Found: C, 48.7%; H, 5.7%; N, 18.6%.$\bar{\nu}_{max}$: 3435, 3134 (O–H), 1626 (COO_{asym}), 1556 (C–N, C=N), 1456, 1418 (C–H), 1392 (COO_{sym}) cm^{-1}. λ_{max}: 230 nm.

$[Fe(C_{12}H_{15}N_4O_2)_2] \cdot 3H_2O$, **5**. 'Mohr salt' $(NH_4)_2Fe(SO_4)_2 \cdot 6H_2O$ (94.3 mg, 0.240 mmol) was added in 6 mL of water/methanol 1:3 v/v solution, while Hbdmpza (31.0 mg, 0.125 mmol) in 4.5 mL NaOH (0.033 M). The ligand mixture was slightly heated to dissolve the solid. The colourless ammonium iron sulphate solution was poured through the filter paper (to remove the remaining solids) into the ligand solution. Pale green crystals of **5** started to appear from the colourless solution at ambient temperature after two days. The reaction mixture was then left at 8 °C, and the crystalline product was filtered off after a week and dried on air for 3 hours. Yield: 61 mg (42%). Anal. Calcd. for $C_{24}H_{36}FeN_8O_7$: C, 47.7%; H, 6.0%; N, 18.5%. Found: C, 48.6%; H, 5.8%; N, 18.3%.$\bar{\nu}_{max}$: 3441 and 3132 (O–H), 1623 (COO_{asym}), 1557 (C–N, C=N), 1458 and 1418 (C–H), 1393 (COO_{sym}) cm^{-1}. λ_{max}: 232, 310 (shoulder) nm.

2. 2. Physical Measurements

CHN elemental analyses were performed by a PERKIN ELMER Elemental Analyzer Series ll CHNS/O.

The infrared spectra of the solid samples were measured in a region between 4000–600 cm^{-1} using a Perkin-Elmer Spectrum 100 series FT-IR spectrometer equipped with Specac Golden Gate ATR as a sample support.

The electronic spectra were measured between 950–200 nm using Perkin-Elmer Lambda 750, UV-Vis-NIR Spectrometer. Each finely ground solid sample was homogenized with nujol oil and the resulting suspension was smeared on a filter paper band. The band was transferred to quartz cuvette (1 cm). Filter paper with nujol oil only was used as a reference.

X-ray powder diffraction data were collected on Panalytical X'Pert PRO MPD powder diffractometer equipped with Ge(111) Johannson type monochromator, in reflection mode using CuKa1 radiation and the full range of the 128 channel linear RTMS detector.

Single crystal diffraction data were collected on an Agilent SuperNova (Dual, Cu at zero, Atlas) diffractome-

ter using Mo Kα radiation at 150 K for **4** and **5**, and at ambient temperature for **1–3**. Data reduction and integration were performed with the software package *CrysAlis PRO*.[12] The coordinates of non-hydrogen atoms were found *via* direct methods using the structure solution program *SIR*97.[13] A full-matrix least-squares refinement on F^2 magnitudes with anisotropic displacement parameters for all non-hydrogen atoms using *SHELXL*-97 was employed.[14] All hydrogen atoms were initially located in difference Fourier maps with exception of those on symmetry disordered water molecules in trihydrates **4** and **5**. However, C-bonded hydrogens were subsequently treated as riding atoms at geometrically idealized positions with bond lengths C–H of 0.98/0.96 Å for methyl, 1.00/0.98 Å for methine and 0.95/0.93 Å for aromatic C–H bonds (the first value corresponds to low temperature and the second to room temperature structure determination). The corresponding displacement parameters U_{iso}(H) were 1.5-times higher than those of the carrier methyl carbons and 1.2-times higher than all other hydrogen bearing carbon atoms.

Table 1. Crystal data, data collection and refinement for **1**–**5**.

Crystal data	**1**	**2**	**3**	**4**	**5**
Formula	$C_{24}H_{34}CoN_8O_6$	$C_{24}H_{34}N_8NiO_6$	$C_{24}H_{34}N_8O_6Zn$	$C_{24}H_{36}MnN_8O_7$	$C_{24}H_{36}FeN_8O_7$
M_r	589.52	589.30	595.96	603.55	604.46
Cell setting, space group	Triclinic, *P*–1	Triclinic, *P*–1	Triclinic, *P*–1	Monoclinic, *C*2/*c*	Monoclinic, *C*2/*c*
a (Å)	7.7536(7)	7.7378(3)	7.7688(4)	16.1601(4)	16.1620(3)
b (Å)	8.6915(7)	8.7338(6)	8.6831(6)	13.3103(3)	13.3097(2)
c (Å)	11.1778(8)	11.0433(6)	11.2345(6)	13.9679(4)	13.9711(2)
α (°)	67.681(7)	67.766(6)	67.747(6)	90	90
β (°)	85.554(6)	85.203(4)	85.591(4)	109.055(3)	109.089(2)
γ (°)	86.834(7)	87.043(4)	86.889(5)	90	90
V (Å^3)	694.48(10)	688.24(7)	699.07(7)	2839.81(13)	2840.08(8)
Z	1	1	1	4	4
D_x (g cm^{-3})	1.410	1.422	1.416	1.407	1.414
μ (mm^{-1})	0.671	0.758	0.931	0.521	0.588
F(000)	309	310	312	1268	1272
Crystal form, colour	Prism, orange	Prism, violet	Prism, colourless	Prism, colourless	Prism, colourless
Crystal size (mm)	0.30 × 0.25 × 0.15	0.45 × 0.30 × 0.30	0.35 × 0.25 × 0.15	0.45 × 0.20 × 0.20	0.30 × 0.20 × 0.15
Data collection					
Temperature (K)	293	293	293	150	150
Radiation type, wavelength	Mo Kα, 0.71073 Å	Mo Kα, 0.71073 Å	Mo Kα, 0.71073 Å	Mo Kα, 0.71073 Å	Mo Kα, 0.71073 Å
Diffractometer	SuperNova, Dual, Cu at zero, Atlas	SuperNova, Dual, Cu at zero, Atlas	SuperNova, Dual, Cu at zero, Atlas	SuperNova, Dual, Cu at zero, Atlas	SuperNova, Dual, Cu at zero, Atlas
Data collection method	ω scans	ω scans	ω scans	ω scans	ω scans
Absorption correction	multi-scan	multi-scan	multi-scan	multi-scan	multi-scan
No. of measured, independent and observed reflections	5761, 3183, 2623	6389, 3146, 2830	5811, 3207, 2774	8006, 3255, 2692	8163, 3257, 2557
Criterion for observed reflections	$F^2 > 2.0\ \sigma(F^2)$	$F^2 > 2.0\ \sigma(F^2)$	$F^2 > 2.0\ \sigma(F^2)$	$F^2 > 2.0\ \sigma(F^2)$	$F^2 > 2.0\ \sigma(F^2)$
R_{int}	0.0308	0.0371	0.0275	0.0263	0.0377
θ range (°)	3.20–27.48	3.20–27.48	3.19–27.48	2.80–27.48	3.06–27.48
h range	–10 → 8	–10 → 9	–10 → 9	–20 → 16	–20 → 16
k range	–11 → 7	–11 → 11	–11 → 7	–17 → 12	–17 → 17
l range	–14 → 13	–14 → 12	–14 → 14	–17 → 18	–13 → 18
Refinement					
Refinement method	Full matrix least-squares on F^2	Full matrix least-squares on F^2	Full matrix least-squares on F^2	Full matrix least-squares on F^2	Full matrix least-squares on F^2
R (on F_{obs}), *wR* (on F_{obs}), *S*	0.0426, 0.1006, 1.045	0.0354, 0.0894, 1.038	0.0380, 0.0911, 1.023	0.0436, 0.1110, 1.082	0.0504, 0.1291, 1.035
No. of contributing reflections	3183	3146	3207	3255	3257
No. of parameters	190	191	190	194	193
No. of restraints	0	1	1	2	0
$(\Delta/\sigma)_{max}$, $(\Delta/\sigma)_{ave}$	<0.001, <0.001	<0.001, <0.001	0.001, <0.001	<0.001, <0.001	<0.001, <0.001
$\Delta\rho_{max}$, $\Delta\rho_{min}$ (eÅ^{-3})	0.283, –0.320	0.253, –0.281	0.261, –0.374	1.233, –0.405	1.441, –0.410

In case of dihydrates, hydrogens from water molecules were refined independently and a bond length restraint O–H of 0.82(2) Å was applied if necessary. In trihydrates, hydrogens from water molecules were found in the difference Fourier map; their coordinates were not refined while their isotropic displacement parameters were constrained to $U_{iso}(H) = 1.2U_{eq}(O)$.

Figures depicting the structures were prepared by *ORTEP*3 and *Mercury*.[15,16] Crystal data and information on data collection and refinement can be seen in Table 1.

CCDC 1019357–1019361 contain the supplementary crystallographic data for this paper. These data can be obtained free of charge from The Cambridge Crystallographic Data Centre *via* www.ccdc.cam.ac.uk/data_request/cif.

3. Results and Discussion

3. 1. Coordination Molecules

The determined crystal structures of all five title compounds consist of homoleptic $[M^{II}(bdmpza)_2]$ coordination molecules (Fig. 1) and water molecules residing among them. Each bdmpza ligand is bound tridentately to the central metal ion, *via* two pyrazole nitrogen atoms and one deprotonated oxygen atom from the carboxylic group in *facial* manner. Such coordination *via* N,O,N sites giving $[M^{II}(\kappa^3\text{-}L)_2]$ is often observed for bdmpza ligand.[1,3] The central metal ion within each structure occupies a special crystallographic position, *i.e.* an inversion centre for **1**–**3**, while a twofold axis for **4** and **5**, respectively. Accordingly, the asymmetric unit comprises one half of the coordination molecule, while two tridentate bdmpza ligands enable a formation of an octahedral environment around the central metal ion. Within the $M^{II}N_4O_2$ chromophore in **1**–**5**, the coordination bond distances do differ to some extent (Table 2, Fig. 2), though less distinguished than in analogous copper compound $[Cu(L)_2] \cdot 2H_2O$,[8] where the basal plane of the coordination octahedron comprises of four nitrogen atoms, while the two oxygen atoms occupy the remaining axial positions, showing longer bond distances due to the Jahn-Teller distortion. Interestingly, the water free copper analogue $[Cu(L)_2]$[8] shows the long N–M–N axis, thus having $M^{II}N_2O_2N_2$ chromophore. Contrary to the hydrated copper compound, the M–O distances in the other hydrates **1**–**5** and related zinc compound $[Zn(L)_2] \cdot 3H_2O$[9] are shorter than their respective M–N distances. The M–N distances in **4**–**5** and $[Zn(L)_2] \cdot 3H_2O$ are almost of the same length, while in **1**–**3** even these bond distances differ, giving them slight compressed or rhombic distorted octahedral character for both groups of compounds, respectively.

Figure 2 shows the differences of the unit cell volume and coordination bonds, respectively, depending on the type of the central metal ion and its ionic radius. The unit cell volume of **4**, **5** and $[Zn(L)_2] \cdot 3H_2O$, which cry-

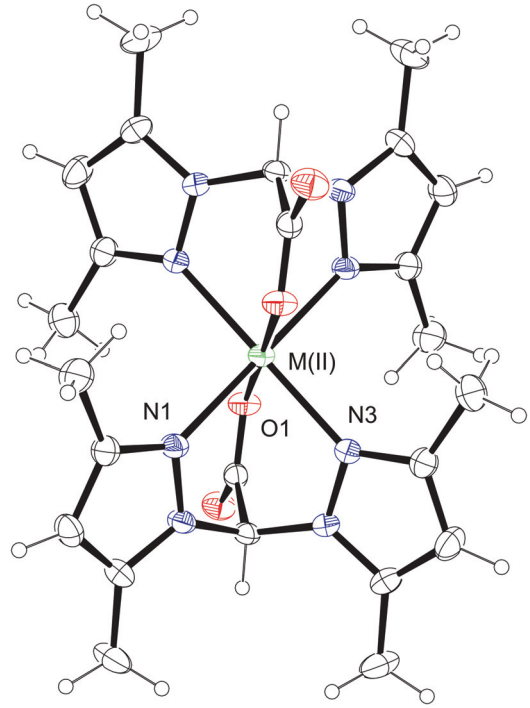

Figure 1. The coordination molecule $[M^{II}(bdmpza)_2]$ in **1**. The asymmetric unit comprises one half of the presented molecule.

Table 2. Bonding distances within the first coordination sphere of central metal ions in **1**–**5** and their hydrated copper and zinc analogues.[8,9]

$[M(L)_2] \cdot xH_2O$	M–O1 [Å]	M–N1 [Å]	M–N3 [Å]	Ionic radius of M [Å]
Co; x = 2 (**1**)	2.085(2)	2.136(2)	2.118(2)	0.745*
Ni; x = 2 (**2**)	2.058(2)	2.089(2)	2.077(2)	0.69
Cu; x = 2[8]	2.293(2)	2.038(2)	2.013(3)	0.73
Zn; x = 2 (**3**)	2.100(2)	2.161(2)	2.138(2)	0.74
Zn; x = 3[9]	2.119(3)	2.178(3)	2.180(3)	0.74
Mn; x = 3 (**4**)	2.157(2)	2.251(2)	2.252(2)	0.83*
Fe; x = 3 (**5**)	2.099(2)	2.191(2)	2.196(2)	0.78*

*For Co^{2+}, Mn^{2+} and Fe^{2+}, the high-spin configurations were proposed due to prolonged coordination bonds in the title compounds when compared with the literature data.[6,17]

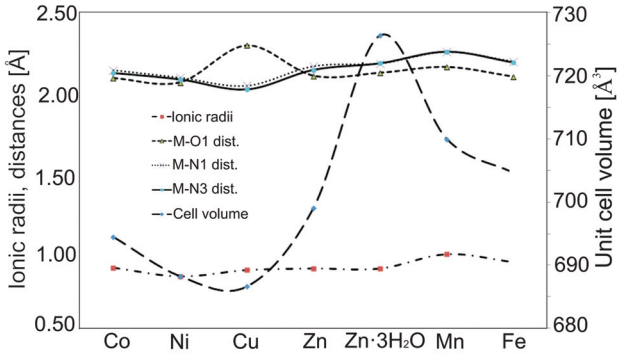

Figure 2. The unit cell volume and M–N and M–O distances [Å] relation with the central metal ion and its radius. The unit cell volumes are normalized.

stallize in a monoclinic cell with $Z = 4$, are approximately four times larger than the triclinic unit cells of **1**–**3** and $[Cu(L)_2] \cdot 2H_2O$ with $Z = 1$ and were thus divided by four for a comparison, *i.e.* normalized. It can be concluded, that with an increase of the atomic radii, all of the aforementioned distances along with the unit cell volumes increase, and vice versa. Additionally, the trihydrates $[M(L)_2] \cdot 3H_2O$ reveal larger unit cell volumes than the dihydrates $[M(L)_2] \cdot 2H_2O$ in relation to more water molecules present as well as their longer average coordination bond distances. The Jahn-Teller distortion is clearly shown in Figure 2, revealing copper compound especially differing at the coordination bond lengths. Its ground state is typical with $d(x^2–y^2)^1$ and $d(z^2)^2$, while more spherical influence of the ligands towards *d* orbital occupancy, for the other metal species investigated herein, is noticed. Such characteristic copper(II) phenomenon may be related with clear ease of copper(II) species isolation, perhaps being the principal activation driving force.

3. 2. Dihydrates $[M(L)2] \cdot 2H_2O$; 1, 2, 3

In the crystal structure of the dihydrates **1**, **2** and **3**, besides one half of the coordination molecule, one symmetry independent molecule of water is present. Thus, between the two adjacent coordination molecules, two net water molecules are positioned, being linked with four hydrogen bonds O–H···O of moderate strength. As being so on each of the two sides, infinite chains are therefore formed (Fig. 3a). Details on hydrogen bond geometry are collected in Table 3.

The packing of the infinite chains being further inter-connected *via* weak intermolecular C–H···C van der Waals interactions is presented in Fig. 3b.

3. 3. Trihydrates $[M(L)2] \cdot 3H_2O$; 4, 5

The first and probably the most obvious difference between di- and trihydrates from the crystallographic point of view is the change of unit cell from triclinic *P*–1

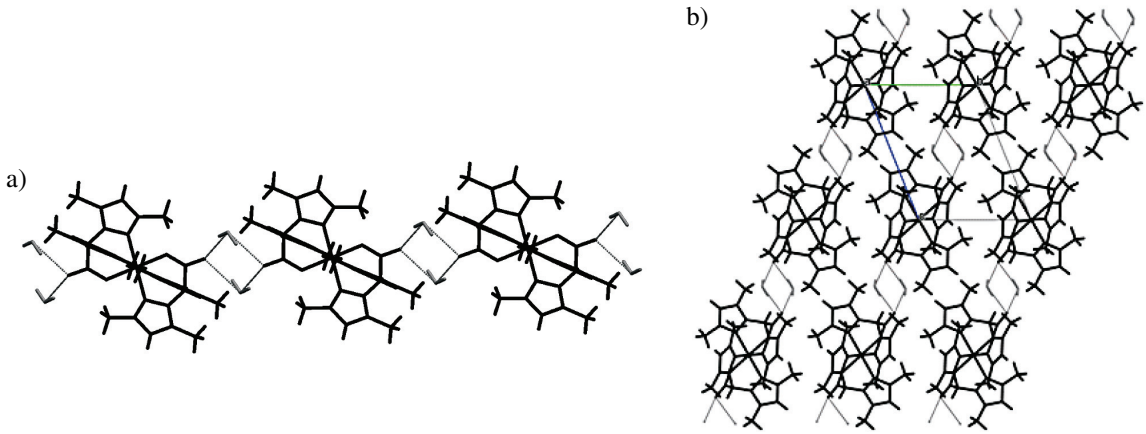

Figure 3. (a) The formation of $[M^{II}(bdmpza)_2] \cdot 2H_2O$ infinite chains with the assistance of O–H...O hydrogen bonds in dihydrate **1**. (b) The packing of infinite chains running along 011 direction in the structures of dihydrate **1**.

Table 3. Details on hydrogen bonding geometry (Å, °) in dihydrates **1–3**.

Compd	D–H...A	D–H	H...A	D...A	D–H...A	Symm. op.
1	O3–H3WA...O2	0.85(5)	2.06(5)	2.844(3)	153(5)	*x*, *y*, *z*
1	O3–H3WB...O2	0.80(4)	2.18(4)	2.922(3)	155(4)	–*x*, –*y*+1, –*z*+1
2	O3–H3WA...O2	0.817(19)	2.09(3)	2.843(3)	154(5)	*x*, *y*, *z*
2	O3–H3WB...O2	0.84(3)	2.12(4)	2.919(3)	161(3)	–*x*, –*y*+1, –*z*+1
3	O3–H3WA...O2	0.83(4)	2.06(4)	2.844(3)	156(4)	*x*, *y*, *z*
3	O3–H3WB...O2	0.808(18)	2.16(2)	2.924(3)	158(3)	–*x*, –*y*+1, –*z*+1

with $V \sim 700$ Å^3 to the monoclinic *C*2/*c* with $V \sim 2800$ Å^3. From the first sight onwards, it must be related with an inclusion of an additional water molecule into the crystal lattice. In **4** and **5**, therefore, two symmetry independent water molecules, namely O3 and O4, appear (in dihydrates, only one with occupancy 1, *i.e.* O3, is present per one half of $[M(L)_2]$). The first one in the trihydrates (occupancy 1) is disordered over two positions (O3a and O3b) with relative occupancies 0.799(4):0.201(4) in **4** and 0.758(4):0.242(4) in **5**, respectively, while the O4 is symmetry disordered, being positioned at a close vicinity of the twofold axis (occupancy 0.5).

The role of O3a in **4** and **5** is almost the same as the role of water O3 in the dihydrates. Namely, within these ~80% of the unit cells, where water O3a is present and O3b is absent, the same building motif, *i.e.* infinite chains of the coordination molecules bridged by two water molecules as in the dihydrates **1**–**3**, appear (see Fig. 3). Additionally to the dihydrates feature, these chains are differently further inter-connected *via* symmetry disordered water molecules O4 into supramolecular layered structure (Fig. 4). The details on hydrogen bonding in trihydrates **4** and **5** are in Table 4.

Considering the ~20% of the unit cells in **4** and **5**, where only O3b is present, a hydrogen bond to the carboxylate O2 atom from the adjacent coordination molecule is formed (Fig. 5). Two O3b water molecules per coordination molecule are attached this way. Another water molecule (*i.e*. the symmetry disordered O4) is hydrogen bonded to this structural segment. Sections consisting of a

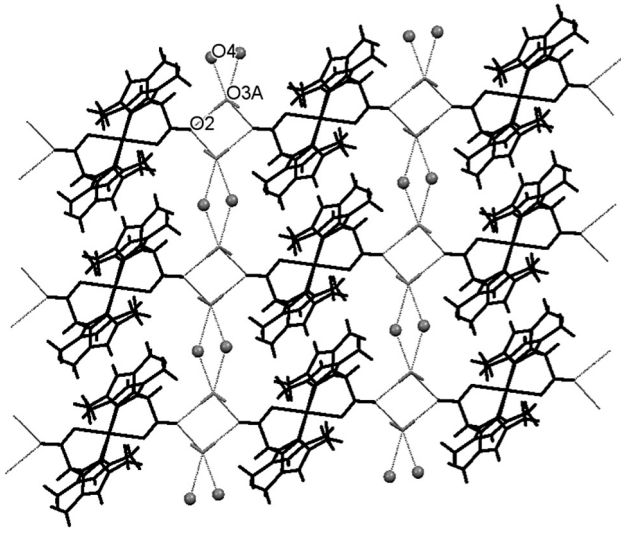

Figure 4. Hydrogen bonding in **4**, considering the presence of O3a (site occupancy ~80%). Extended supramolecular sheets are formed due to hydrogen bonding between the parallel infinite chains *via* symmetry disordered O4 water.

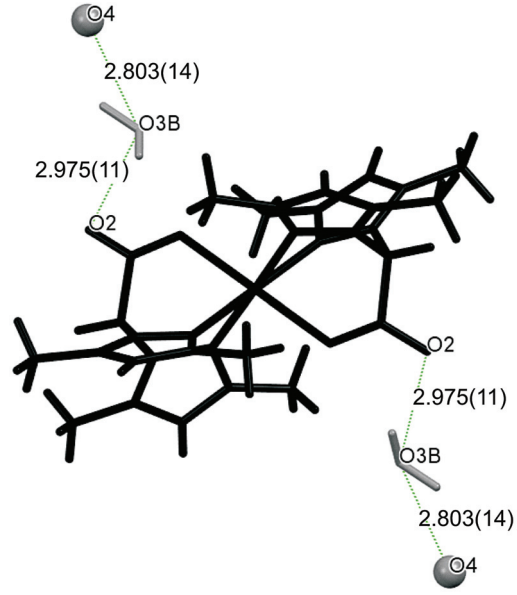

Figure 5. Hydrogen bonding in **4**, considering the presence of O3b site (occupancy ~20%). Two pairs of water molecules are hydrogen bonded to the isolated coordination molecules.

Table 4. Hydrogen bond geometry (Å, °) in trihydrates **4** and **5**.

Compd	D–H···A	D–H	H...A	D...A	D–H...A	Symm. op.
4	O3A–H3A1...O2	0.94	1.92	2.837(3)	162.1	*x*, *y*, *z*
4	O3A–H3A2...O2	0.90	2.04	2.942(3)	175.1	–*x*+3/2, –*y*+1/2, –*z*
4	O3B–H3B1...O2	0.80	2.27	2.975(11)	146.9	*x*, *y*, *z*
4	O4...O3A	–	–	2.683(8)	–	*x*, *y*, *z*
4	O4...O3A	–	–	2.882(7)	–	1–*x*, *y*, –*z*–1/2
4	O3B –H3B2....O4	1.02	2.01	2.803(14)	133.0	*x*, *y*, *z*
5	O3A–H3A1...O2	0.94	1.93	2.854(4)	166.3	*x*, *y*, *z*
5	O3A–H3A2...O2	0.90	2.08	2.985(4)	174.1	–*x*+3/2, –*y*+1/2, –*z*
5	O3B–H3B1...O2	0.80	2.22	2.943(11)	149.2	*x*, *y*, *z*
5	O4...O3A	–	–	2.694(11)	–	*x*, *y*, *z*
5	O4...O3A	–	–	2.947(11)	–	1–*x*, *y*, –*z*–1/2
5	O3B –H3B2...O4	1.02	1.98	2.784(16)	133.8	*x*, *y*, *z*

*Since hydrogen atoms on O4 were not determined, only O4...O3A distance is given. Due to the 'dihydrate' O3a water H-bonding, it is expected that O4 is a hydrogen bond donor.

coordination molecule and two pairs of water molecules (O4, occupancy 0.5) are thus obtained in ~20% of the unit cells (Fig. 5).

This analogy of both stable hydrate structural types, differing in water H-bonding networks, is further confirmed by the XRD powder analysis. It shows almost identical features within each group, though clear difference among all (see Supplementary Information). The measured zinc powder XRD reveals a presence of both, *i.e.* di- and trihydrate, showing both species may be obtained at similar conditions, possibly in relation with a very stable zinc(II) oxidation state. The network water molecules thus generally enable stable different types of packing. However, it seems the network water molecules do not activate additionally the catalytic potential of the coordination species by their impact towards the first coordination sphere, since this sphere remains closely sealed octahedral ML_6; $[MN_4O_2]$. It was deformed only within the copper species $[MO_2N_2O_2]$. Another alternative for this issue would be very welcome, probably *via* another solvent and counterion.

Interestingly, in the structures of Mg and Zn trihydrate analogues,[9,10] the O4 water was symmetrically disordered, while O3 was not disordered at all. It is important to stress once again that the hydrogen atoms attached to O4 in Zn trihydrate compound[9] were not observed in the difference Fourier map, while those on O3 were, refined one by one with the appropriate bond length restraints and fixed at the final refinement cycles due to high shifts/unstable refinement.

3. 3. Spectroscopy

Figure 6 shows the infrared spectra of the compounds **1**–**5** and copper dihydrate analogue. At first glance, the vibrational spectra of all six compounds are very similar. However, a detailed view shows almost identical feature for **4** and **5** on one hand, as well as the spectra of **1**–**3** and related copper species on the other hand, respectively. Most obvious-differences among both groups of compounds are seen in the shapes of O–H stretching absorptions around ~3300 cm^{-1} and asymmetric stretching absorptions of the carboxylate group at 1650 cm^{-1}. In case of the dihydrates **1**–**3**, there are two ν(O–H) bands that are well-resolved. For the trihydrates **4**–**5**, in which hydrogen

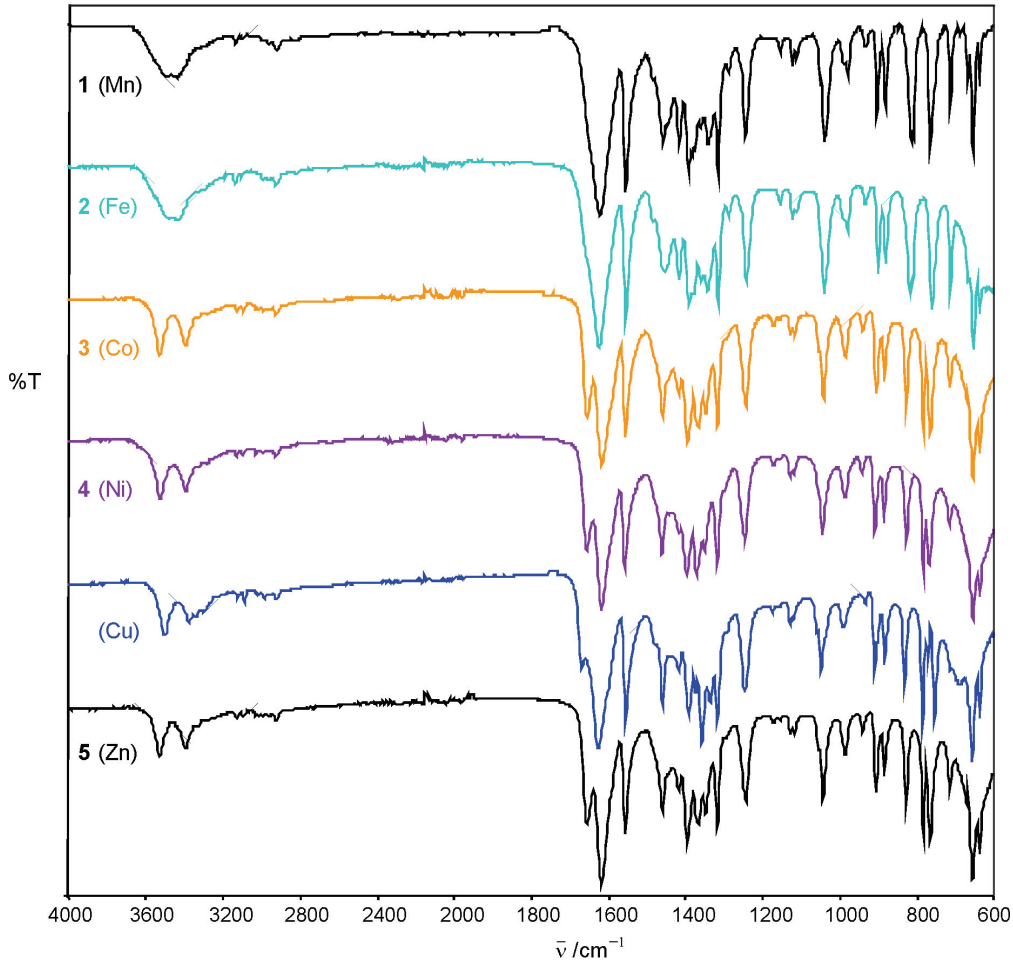

Figure 6. IR spectra of **1**–**5** and their copper hydrated analogue $[M^{II}(bdmpza)_2]$.

bonding is more diverse, the aforementioned bands get broader and are not resolved to the distinguished lines anymore. Similar phenomenon can be observed at approximately twice smaller energy as due to the asymmetric carboxylate stretching absorptions, where an additional band can be observed for the title dihydrates and one broad band for the respective trihydrates.

The electronic spectra are in accordance with the metal oxidation states and ligands attached.[18] As such, they are not significantly related with the water arrangement outside the coordination sphere.

4. Conclusions

Five new coordination compounds with the common formulae $[M^{II}(bdmpza)_2]\cdot xH_2O$ (bdmpza = bis(3,5-dimethylpyrazol-1-yl)acetate, Co (**1**), Ni (**2**), Zn (**3**), Mn (**4**) and Fe (**5**) were isolated and compared with the other two known species in this system, namely $[Cu^{II}(bdmpza)_2] \cdot 2H_2O$[8] and $[Zn^{II}(bdmpza)_2] \cdot 3H_2O$.[9] The typical octahedral coordination sphere is found in all cases showing only small differences among each other. Interestingly, the expectedly weaker stabile Mn^{II} (**4**) and Fe^{II} (**5**) species[19,20] were isolated as trihydrates, Co (**1**), Ni (**2**) and Cu[8] as dihydrates, while Zn as di-(**3**) and trihydrate.[9] The two stable hydrate groups are distinguished with obvious resemblance (even isostructurality) also at the powder XRD and IR analysis. All trihydrates clearly show longer coordination bonds, along with the expected larger unit cell volume (more net water molecules). Ionic radius thus seems to be important, though solely shell does not favour any kind of the hydrate, as both types were isolated with zinc. Also the reaction conditions may not be the decisive reason for the diferenciation, due to many alternative procedure tryouts, but only limited number of the final products for each late 3d metal. It seems more probable that alternative hydrate types are plausible *in situ* as the partial motif of the dihydrates is found also within one of the trihydrate structural patterns. Both, namely the dihydrate and trihydrate type, or even more alternative pathways (*e.g.* a and b trihydrate) are thus simultaneously competing by packing the same available structural building blocks. More disordered option, namely trihydrate type, seems to enable additional stabilization to the oxygen sensitive Mn^{II} and Fe^{II} species, while firmly stable Zn^{II} can adopt either of the two forms.

5. Acknowledgements

The authors thank Katja Mikolič for the synthesis, the Slovenian research agency ARRS (grant P1-0175) for the financial support and EN-FIST 'Centre of excellence' for access to SuperNova single crystal diffractometer.

6. References

1. S. Trofimenko, *Scorpionates, The Coordination Chemistry of Polypyrazolylborate Ligands*, Imperial College Press, London, UK, **2005**.
2. *Concepts and models in bioinorganic chemistry,* 3. ed., Eds., H.-B. Kraatz, N. Metzler-Nolte, Wiley-VCH, Weinheim, **2006**.
3. C. Pettinari, R. Pettinari, *Coord. Chem. Rev.* **2005**, *249*, 663–691. http://dx.doi.org/10.1016/j.ccr.2004.08.017
4. N. Burzlaff, *Advances in Inorganic Chemistry*, **2008**, *60*, 101–165.
5. N. Kitanovski, N. Borsan, M. Kasunic, V. Francetic, J. Popovic, I. Djerdj, X. Rocquefelte, J. Reedijk, B. Kozlevcar, *Polyhedron* **2014**, *70*, 119–124. http://dx.doi.org/10.1016/j.poly.2013.12.029
6. F. H. Allen, *Acta Crystallogr. B* **2002**, *58*, 380–388. http://dx.doi.org/10.1107/S0108768102003890
7. N. Burzlaff, I. Hegelmann, B. Weibert, *J. Organomet. Chem.* **2001**, *626*, 16–23. http://dx.doi.org/10.1016/S0022-328X(01)00648-9
8. B. Kozlevcar, P. Gamez, R. de Gelder, W. L. Driessen, J. Reedijk, *Eur. J. Inorg. Chem.* **2003**, 47–50. http://dx.doi.org/10.1002/ejic.200390005
9. A. Beck, B. Weibert, N. Burzlaff, *Eur. J. Inorg. Chem.* **2001**, 521–527. http://dx.doi.org/10.1002/1099-0682(200102)2001:2<521::AID-EJIC521>3.0.CO;2-Q
10. V. Chandrasekhar, P. Thilagar, T. Senapati, *Eur. J. Inorg. Chem.* **2007**, 1004–1009. http://dx.doi.org/10.1002/ejic.200600978
11. B. Kozlevcar, P. Gamez, R. de Gelder, Z. Jaglicic, P. Strauch, N. Kitanovski, J. Reedijk, *Eur. J. Inorg. Chem.* **2011**, 3650–3655. http://dx.doi.org/10.1002/ejic.201100410
12. CrysAlis PRO, Oxford Diffraction Ltd: Yarnton, UK, **2011**.
13. A. Altomare, M. C. Burla, M. Camalli, G. Cascarano, C. Giacovazzo, A. Guagliardi, A. G. G. Moliterni, G. Polidori, R. Spagna, SIR97, *J. Appl. Crystallogr.* **1999**, *32*, 115–119. http://dx.doi.org/10.1107/S0021889898007717
14. G. M. Sheldrick, *Acta Crystallogr. A* **2008**, *64*, 112–122. http://dx.doi.org/10.1107/S0108767307043930
15. L. J. Farrugia, *J. Appl. Crystallogr.* **1997**, *30*, 565. http://dx.doi.org/10.1107/S0021889897003117
16. C. F. Macrae, P. R. Edgington, P. McCabe, E. Pidcock, G. P. Shields, R. Taylor, M. Towler, J. van De Streek, *J. Appl. Crystallogr.* **2006**, *39*, 453–457. http://dx.doi.org/10.1107/S002188980600731X
17. R. D. Shannon, *Acta Crystallogr. A* **1976**, *32*, 751–767. http://dx.doi.org/10.1107/S0567739476001551
18. A. B. P. Lever, *Inorganic Electronic Spectroscopy*, Elsevier, Amsterdam, The Netherlands, **1984**.
19. M. Wekesa, M. J. Uddin, H. F. Sobhi, *Int. J. Chem. Res.* **2011**, *2*, 34–37.
20. B. Morgan, O. Lahav, *Chemosphere* **2007**, *68*, 2080–2084. http://dx.doi.org/10.1016/j.chemosphere.2007.02.015

Povzetek

Iz reakcijskih zmesi, ki so vsebovale ustrezno kovinsko sol, bis(3,5-dimetilpirazol-1-il)ocetno kislino (Hbdmpza), metanol in vodo, smo pripravili pet novih spojin s splošno formulo $[M^{II}(bdmpza)_2] \cdot xH_2O$ (bdmpza = $C_{11}H_{15}N_4COO^-$; x = 2 za Co (**1**), Ni (**2**) in Zn (**3**), x = 3 za Mn (**4**) in Fe (**5**)). Rentgenska strukturna analiza monokristalov je pokazala, da vseh pet spojin (**1**–**5**) vsebuje enojedrne koordinacijske molekule $[M^{II}(bdmpza)_2]$, v katerih je centralni kovinski ion obdan z dvema kelatnima ligandoma; vsak od njiju je koordiniran trivezno na facialni način preko κ^3-*N,N,O* atomov liganda. V dihidratih $[M(L)_2] \cdot 2H_2O$, **1**–**3**, je vsaka koordinacijska molekula povezana preko dveh molekul vode, tj. z dvema paroma O–H···O vodikovih vezi na vsaki strani, kar vodi do nastanka verig. V trihidratih $[M(L)_2] \cdot 3H_2O$, **4**–**5**, se s pomočjo dodatne molekule vode omenjene verige povežejo v supramolekularne plasti. Stabilnost di- in trihidratov smo potrdili z rentgensko praškovno difrakcijo in infrardečo spektroskopijo. Polmer kovinskih ionov in koordinacijske vezi M–O, M–N smo povezali z dimenzijami praznin med koordinacijskimi molekulami obravnavanih spojin $[M^{II}(bdmpza)_2] \cdot xH_2O$.

Supplementary information (SI) - XRD powder data

(pract – powder diffractogram measurement; teor – calculated diffractogram from the single crystal data)

1 pract (Co, dihydrate)

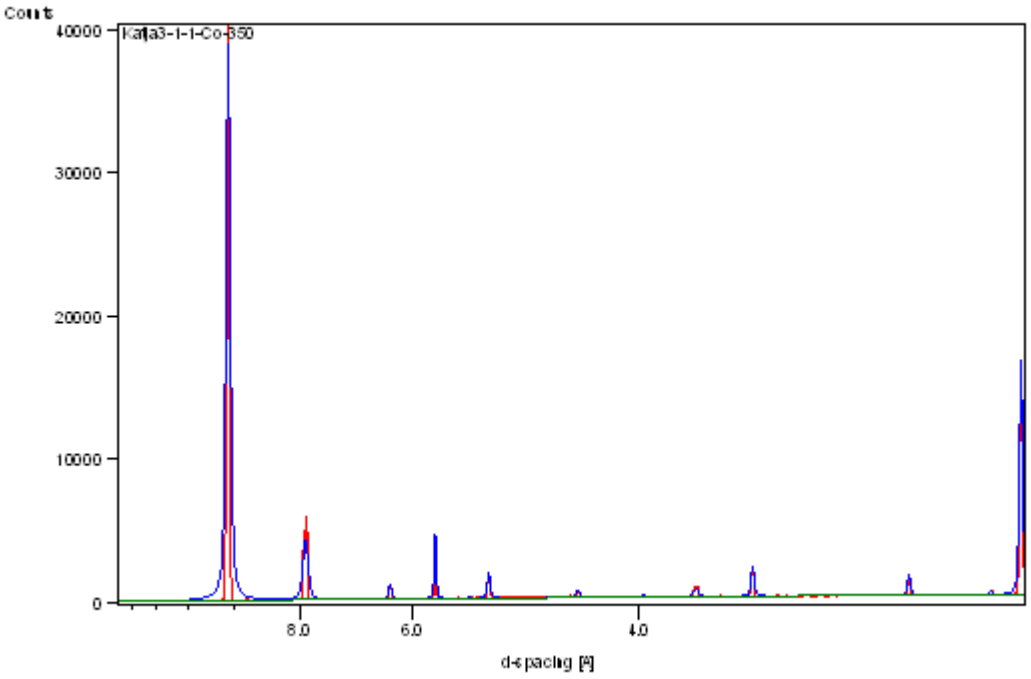

1 teor (Co, dihydrate)

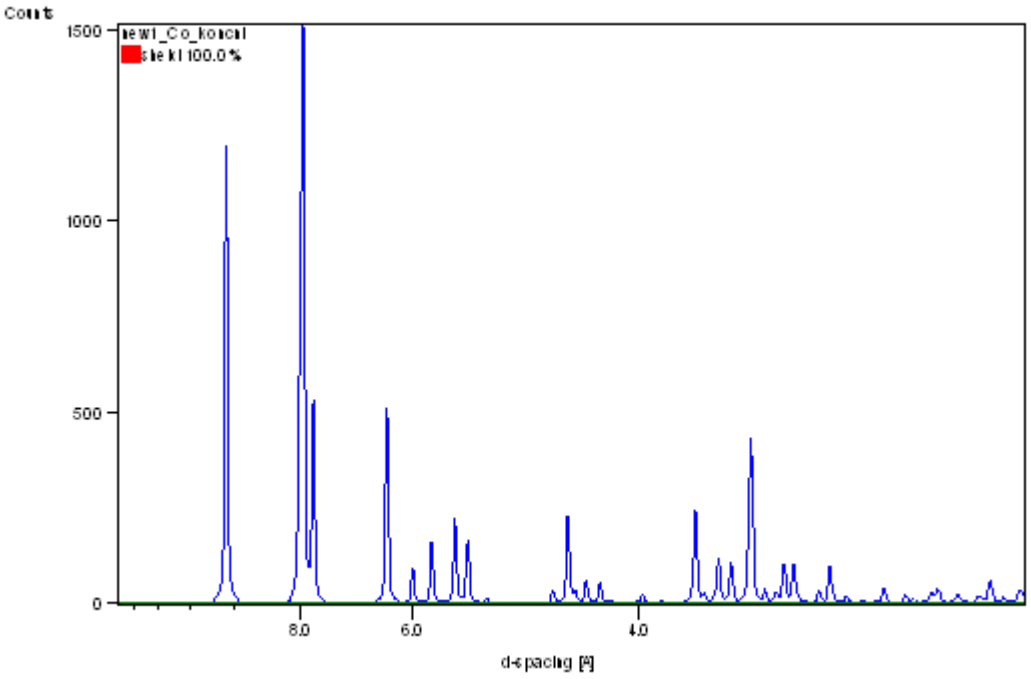

2 pract (Ni, dihydrate)

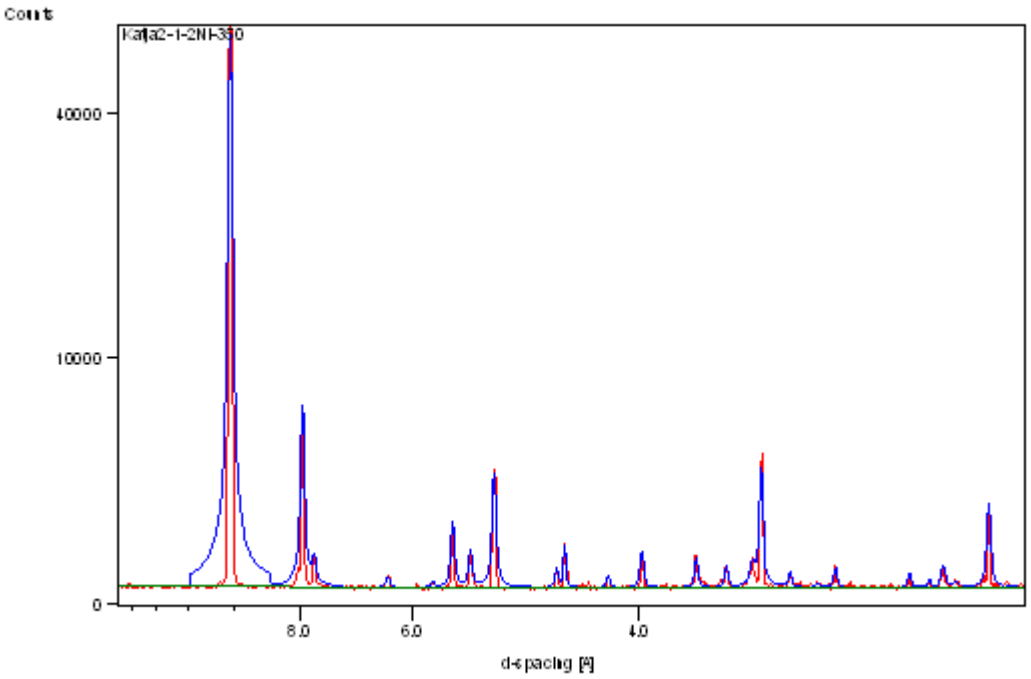

2 teor (Ni, dihydrate)

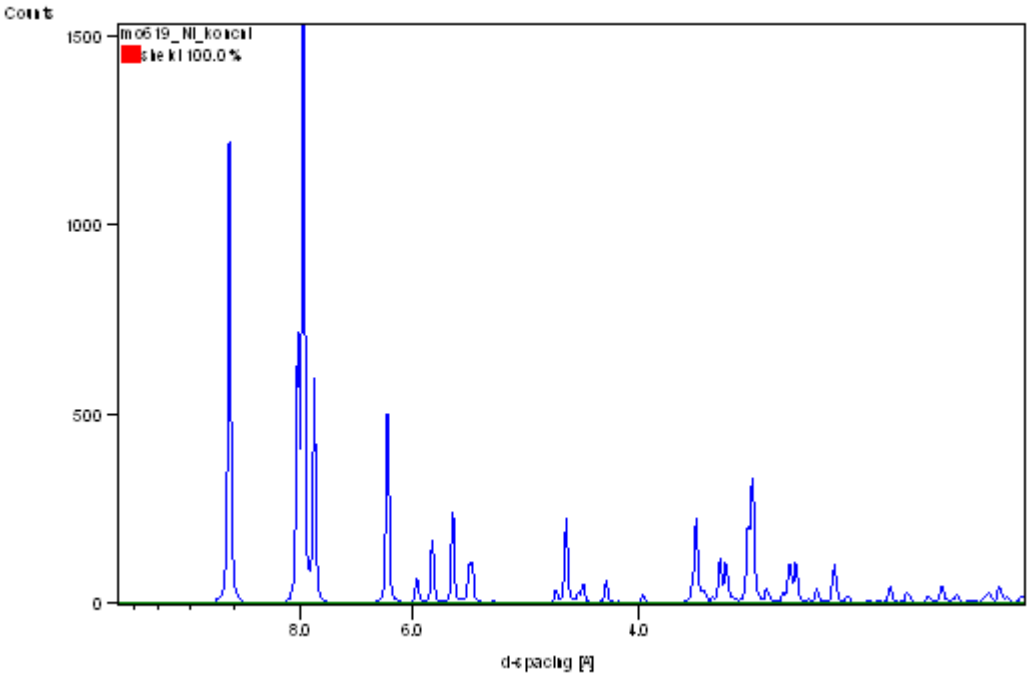

3 pract (Zn, dihydrate)

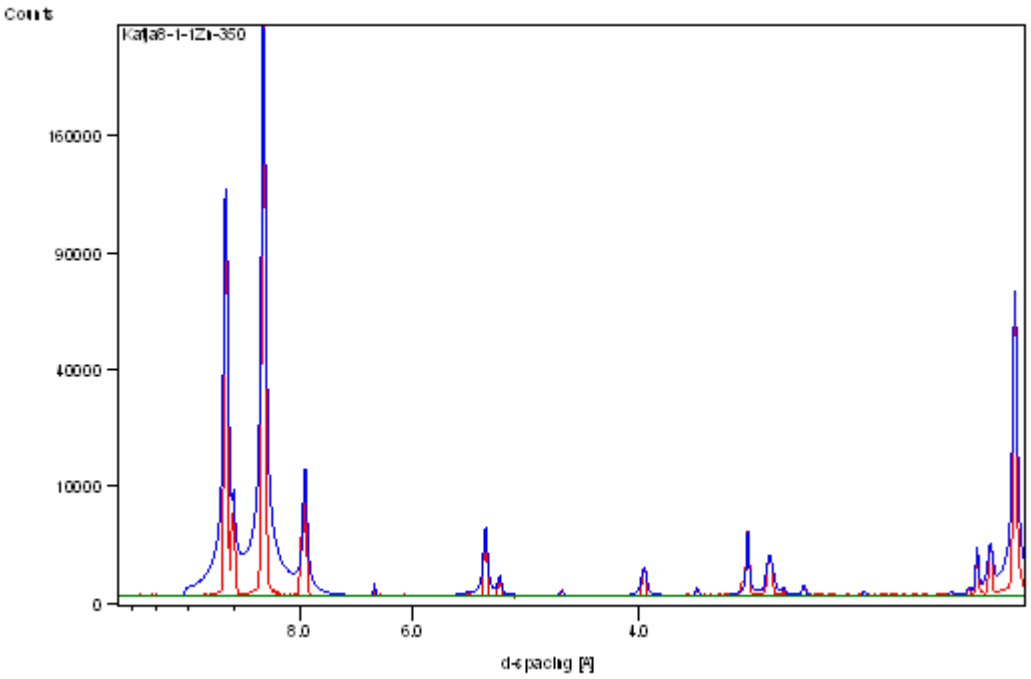

3 teor (Zn, dihydrate)

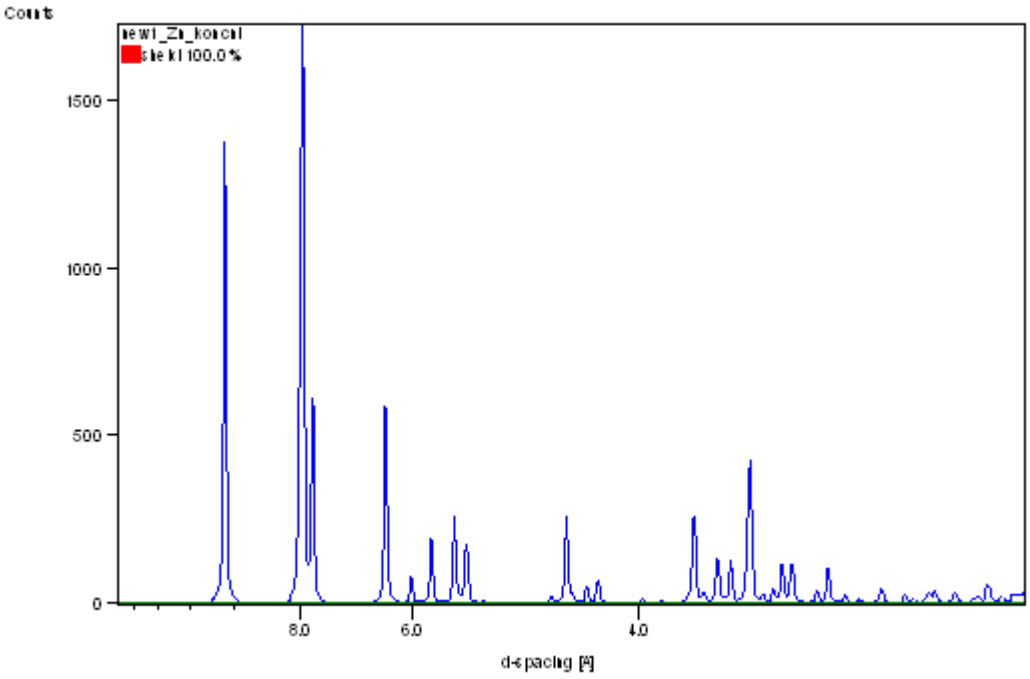

4 pract (Mn, trihydrate)

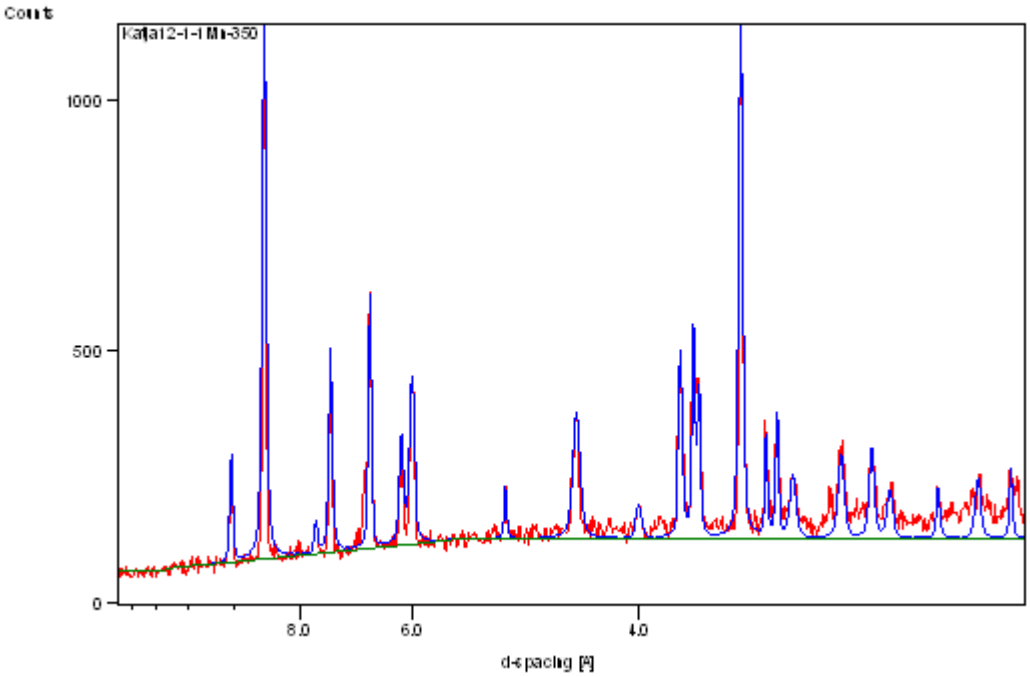

4 teor (Mn, trihydrate)

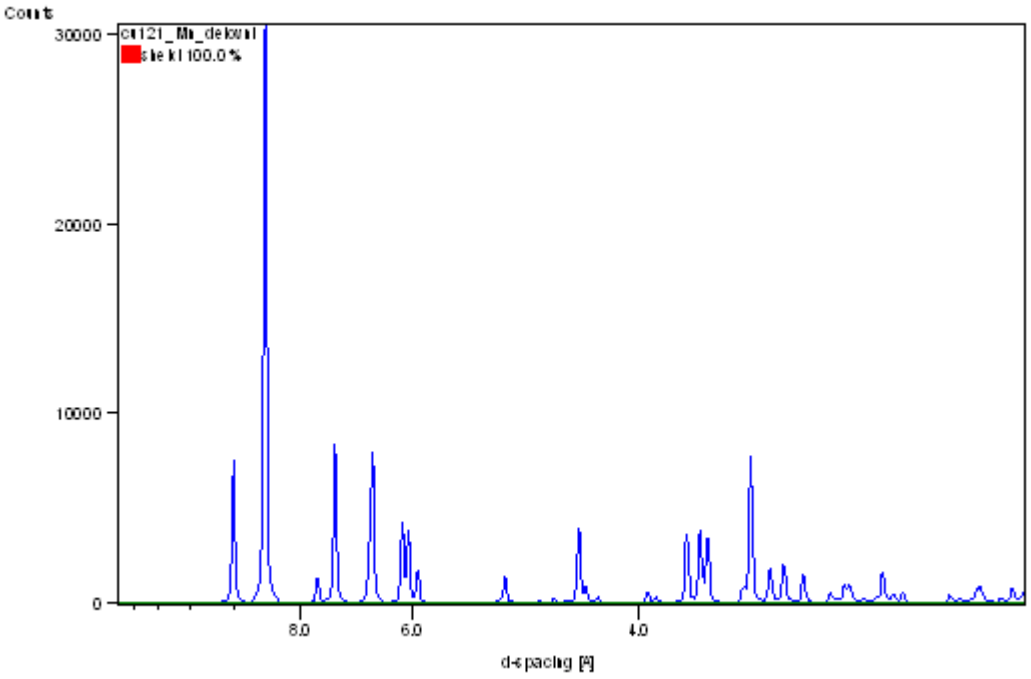

5 pract (Fe, trihydrate)

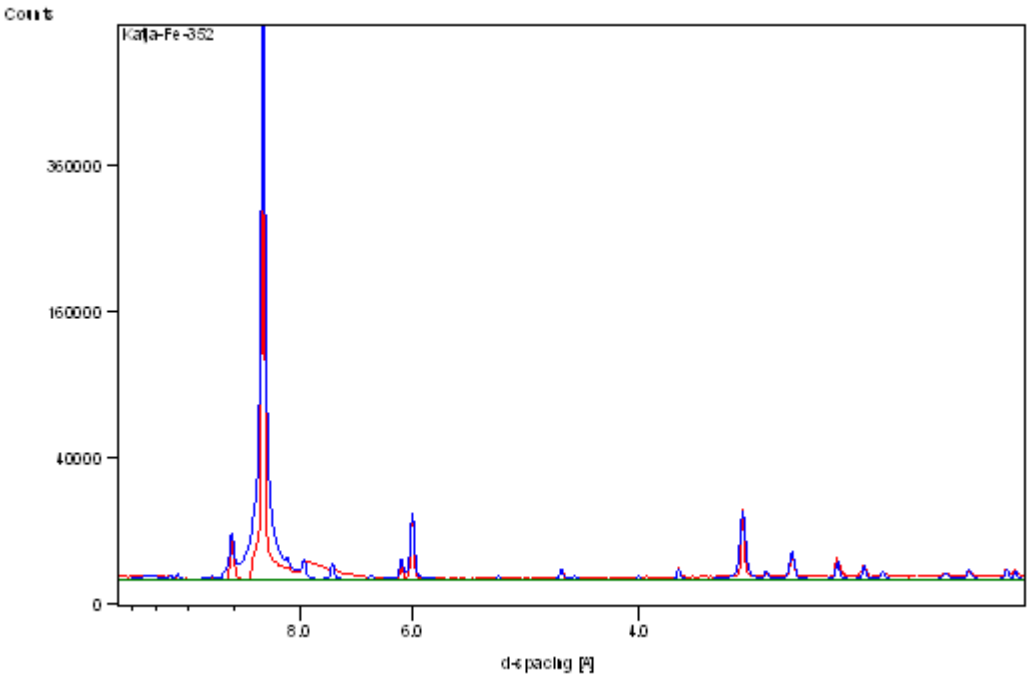

5 teor (Fe, trihydrate)

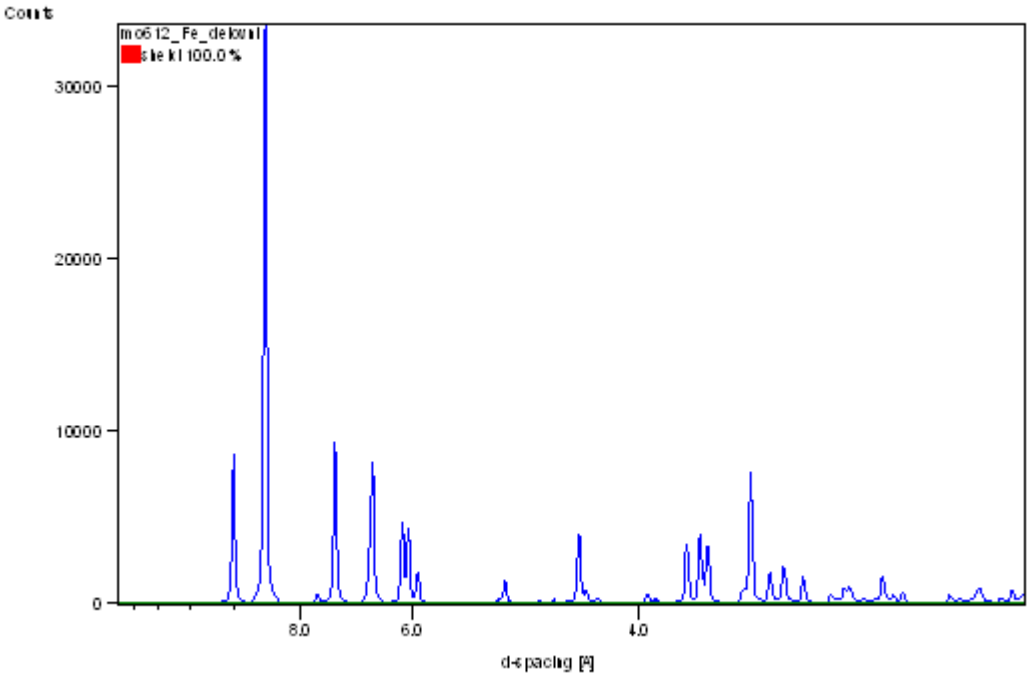

Cu pract (dihydrate)

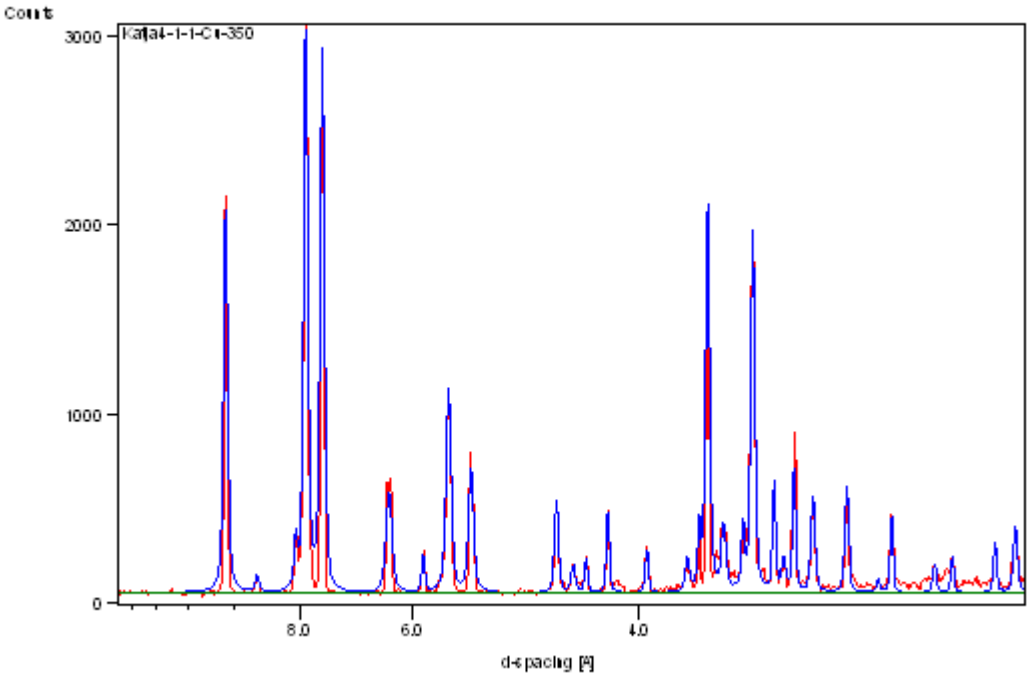

Cu teor (dihydrate)

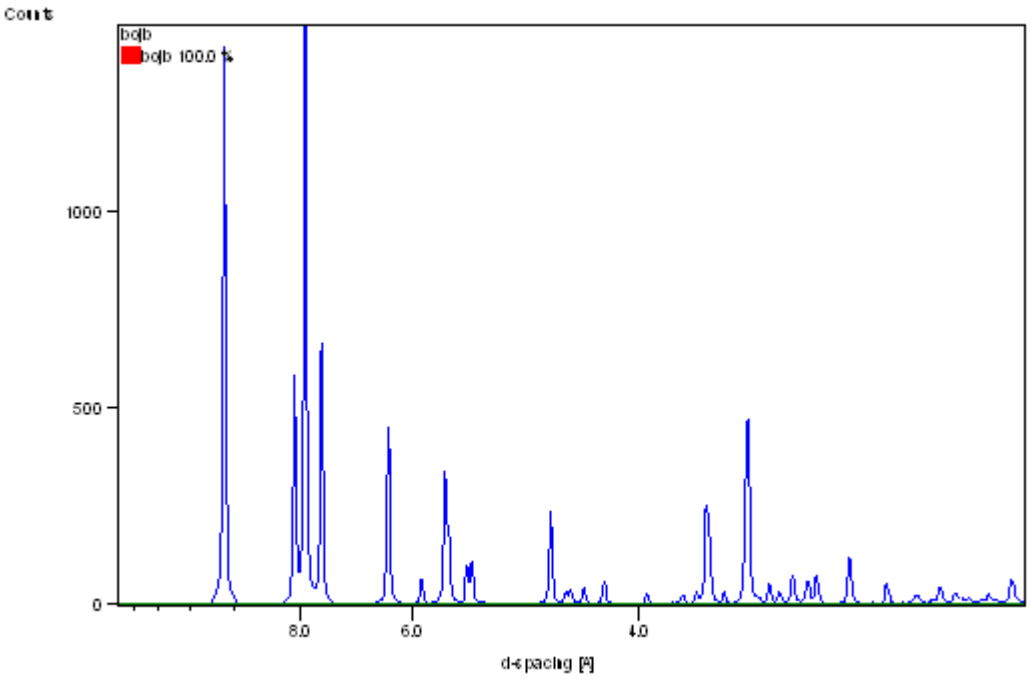
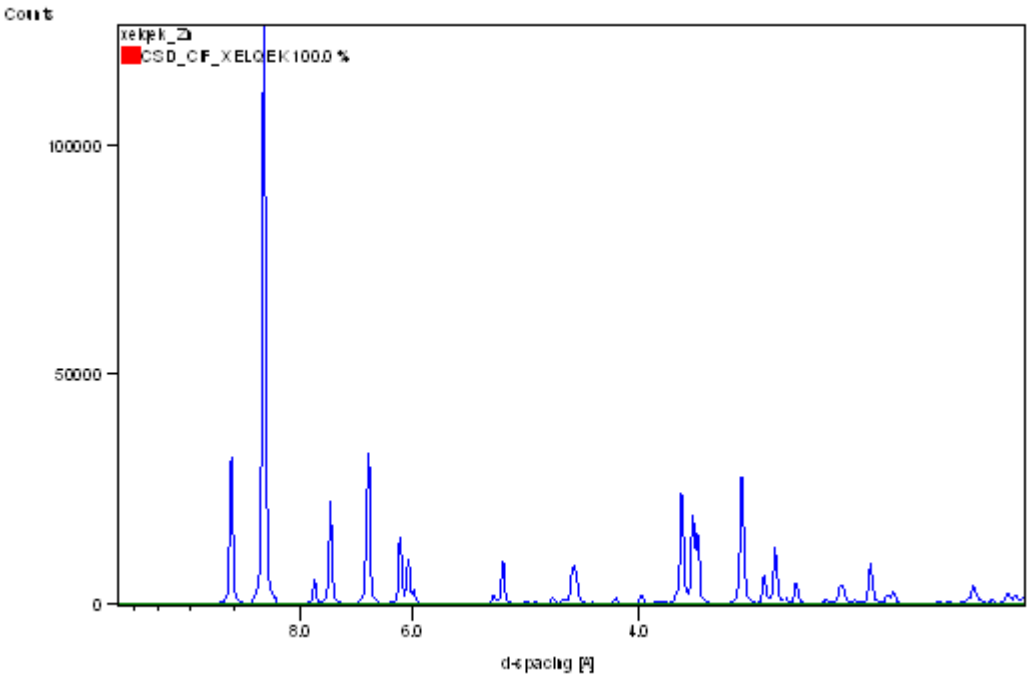
Zn teor (trihydrate)